China Ocean Eng., 2022, Vol. 36, No. 4, P. 575–587
DOI: https://doi.org/10.1007/s13344-022-0051-6, ISSN 0890-5487
http://www.chinaoceanengin.cn/ E-mail: coe@nhri.cn

6-DOF Motion Assessment of A Hydrodynamic Numerical Simulation of A Semisubmersible Platform Using Prototype Monitoring Data

LI Song[a, b], WU Wen-hua[a, b, c, *], YAO Wei-an[a, b]

[a] Faculty of Vehicle Engineering and Mechanics, Dalian University of Technology, Dalian 116024, China

[b] State Key Laboratory of Structural Analysis of Industrial Equipment, Dalian University of Technology, Dalian 116024, China

[c] Research Institute of Dalian University of Technology in Shenzhen Gaoxin South fourth Road, Nanshan District, Shenzhen 518057, China

Received June 12, 2021; revised February 9, 2022; accepted March 18, 2022

Abstract

Hydrodynamic numerical simulations are used to conduct structural analyses and inform the design of engineered marine structures. In this paper, a hydrodynamic numerical model of "Nanhai Tiaozhan" (NHTZ) FPS platform was established according to its design specifications. The model was assessed with two sets of field monitoring data representing harsh and conventional sea states. The motion responses of the platform according to the measured data and the hydrodynamic simulation were compared by reviewing their statistical characteristics, distributions, and spectrum characteristics. The comparison showed that the hydrodynamic model could correctly simulate the frequency domain characteristics of the motion responses of the platform. However, the simulation underestimated the reciprocating motions of the floating body and the influence of slow drift on the motion of the platform. Meanwhile, analysis of the monitoring data revealed that the translational degrees of freedom (DOF) and rotational DOF of the platform were coupled, but these coupled motion states were not apparent in the hydrodynamic simulation.

Key words: prototype monitoring, hydrodynamic numerical simulation, statistical characteristics, semisubmersible platform, reciprocating motions

Citation: Li, S., Wu, W. H., Yao W. A., 2022. 6-DOF motion assessment of a hydrodynamic numerical simulation of a semisubmersible platform using prototype monitoring data. China Ocean Eng., 36(4): 575–587, doi: https://doi.org/10.1007/s13344-022-0051-6

1 Introduction

Hydrodynamic numerical simulations are fundamental to the design of marine structures. US Department of Defense (2020) pointed out these simulations enable the calculation of the motion responses of a platform with six degrees of freedom (6 DOF) and force states within the mooring system. Much research has been carried out to improve the modeling of ocean environmental loads and hydrodynamic simulations (Pedersen, 2012; Feng et al., 2015; Yang et al., 2012; Söylemez and Atlar, 2000). Generally speaking, hydrodynamic analyses use either the time domain method or the frequency domain method. When considering nonlinear waves, Clauss et al. (2003) demonstrated that the results from the time domain method agreed better with experimental results than those from the frequency domain method. Numerical simulation analyses of the hydrodynamic performance of platforms are mainly based on the Morison formula and potential flow theory, and are usually carried out using first-order approximations of velocity potential. However, recent studies have indicated that the effects of second-order wave forces on marine structures, especially mooring structures, should not be ignored.

The hydrodynamics software AQWA uses the Newman method by default to calculate second-order wave forces. However, Chen et al. (2013b) investigated the applicability of second-order wave forces at different water depths, and pointed out that the Newman method was only applicable to deep-water conditions. Furthermore, van Sluijs and Minkenberg (1977) pointed out that low frequency motion in the horizontal plane of a platform had a great influence on stability. Low and Langley (2006) developed a hybrid analysis method that combined the linear frequency domain method with the time domain method to perform a fully-coupled analysis of offshore platform structural stability. However, this fully-coupled analysis still ignored the influence of geo-

Foundation item: This research was financially supported by the National Natural Science Foundation of China (Grant No. U1906233) and the Central Guidance on Local Science and Technology Development Fund of Shenzhen (Grant No. 2021Szvup021).

*Corresponding author. E-mail: lxyuhua@dlut.edu.cn

metric non-linearity on the platform structure. Analyses of the hydrodynamic characteristics of floating platforms are generally conducted using the partial coupling method in marine engineering (Senra et al., 2002). However, the hull, moorings, and risers of offshore platforms form a highly interdependent and nonlinear system with obvious coupled motions and multi-scale effects. Therefore, the hydrodynamic numerical method still needs further investigation and refinement to accurately simulate the motion response of platforms.

Field monitoring systems are commonly deployed to service structures to measure and obtain monitoring data which can then be used in data mining analysis. The monitoring data can provide an important basis on which the performance of large and complex structures under complex loads can be evaluated. In the 1980s, many studies contributed towards establishing structural health monitoring (SHM) systems for various bridge structures (Chen et al., 2013a; Ko and Ni, 2005). Based on monitoring data, static and dynamic analyses of bridge structures were carried out and assessed. The main focal points of these studies were vibration strength, strain response, the modal parameters of bridge structures affected by temperature, wind, traffic, and other load factors (Brownjohn et al., 2015; Kim et al., 2017; Wang et al., 2019; Asadollahi and Li, 2017). Furthermore, SHM has been applied in the aerospace field, for example, Hunt and Hebden (1999, 2001) inferred the remaining service life of a fighter jet using the field monitoring method.

Since 2000, the application of SHM towards marine engineering problems has attracted increasing attention. Edwards et al. (2005) summarized the monitoring projects of 17 deep water floating platforms in the Gulf of Mexico, and introduced the related load and motion monitoring systems. Du et al. (2013, 2014, 2015, 2016) established a prototype monitoring system on the "NHTZ" FPS that measured the hull motion and the forces experienced by the mooring system, and a comprehensive study was carried out on the environmental load conditions in the South China Sea. Leverette et al. (2003) established a top tension monitoring system on the Allegheny Sea-star TLP (Tension Leg Platform) platform in the Gulf of Mexico and inferred the VIV (Vortex-Induced Vibration) and springing phenomena of the tension leg under the action of strong ocean currents by analyzing the field monitoring data. They also noted that the vibration of the tension leg affected the vessel hull. Teigen and Haver (1998) used long-term measurement data obtained on the Heidrum TLP to study the consistency between the measured 6 DOF motions and the design indicators. Their results showed that the designed parameters of the TLP platform were relatively conservative. Perego et al. (2005) compared the measured motions of the Marlin TLP with a fully-coupled numerical analysis based on the measured information. Tahar et al. (2005, 2006) and Halkyard et al. (2004) compared the monitoring results from the Horn Mountain Spar during Typhoon Isidore in the time and frequency domains. Their simulated results showed that it is feasible to make fast and approximate estimations of response statistics using the frequency domain coupling method.

This study was based on the monitoring data from the prototype monitoring system installed on the "NHTZ" FPS. In particular, sets of monitoring data collected during extreme typhoon sea conditions and a set of monitoring data under conventional sea conditions were selected to perform the hydrodynamic numerical simulations. The monitoring system, selected data sets, and simulations are described in Section 2. Then, in Section 3, the hydrodynamic numerical simulation results were compared with the measured field motion responses in regard to the time domain, frequency domain, and statistical characteristics, and the simulated results from the two sea conditions data sets are discussed. Section 4 provides a comparison and analysis of the measured 6-DOF motion data and the hydrodynamic simulation results. A brief summary and discussion are given in Section 5.

2 Field monitoring system of the "NHTZ" FPS

"NHTZ" FPS (Floating Production Storage) is located in the LH11-1 oil field in the South China Sea at an operational water depth of 305 m. Since 2011, a prototype monitoring project of the "NHTZ" FPS has been ongoing, and monitoring data during typhoons and other extreme loading events have been accumulated. The arrangement of sensors in the monitoring system is shown in Fig. 1.

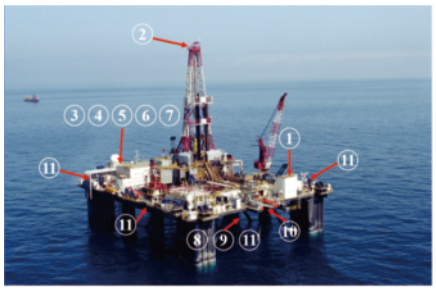

Fig. 1. "NHTZ" FPS prototype monitoring system.

In addition to the 6 DOF motion data of the platform and the underwater inclination data of the mooring system, global monitoring data including data associated with ocean environmental loads like wind, waves, and currents were also collected. Table 1 shows the types, ranges, and accuracies of the sensors used in ocean environment and platform motion monitoring.

In order to comprehensively analyze the motion behaviors of the structure, sets of conditions representing typhoons (Condition 1) and conventional seas (Condition 2) were selected for analysis. The set referred to as Condition 1 was measured during Typhoon "Nock-ten" from 19:30 to 22:30 on July 28, 2011 shown in Table 2. The Condition 2 data set

Table 1 Range and accuracy of monitoring information

Type	Sensor	Information	Range	Accuracy
Wind	Vane anemometer	Wind speed, wind direction	0−100 m/s, 0°−360°	0.1 m/s, 0.2°
Wave	Waveguide radar	Wave height, wave direction, T_p	0−30 m, 0°−360°	0.01 m, 1°
Current	ADCP	Current velocity, current direction	±10 m/s, 0°−360°	0.1 m/s, 1°
Linear motion	DGPS	Sway, surge	>0 m	0.1 m
		Heave	0−3 m	0.1 m
Angular motion	INS	Roll, pitch	±30°	0.01°
		Yaw	0°−360°	0.05°

was the measured load from 16:30 to 19:30 on July 27, 2011, which was the representative of a normal day, shown in Table 3. Where V(3hr@10m) is three-hour mean wind speed at 10 m above the sea level, MeanDir (3hr@10m) is the three-hour mean wind direction relative to the bow at 10 m above the sea level. But due to the limitation of space, the wind speed and direction applied in the actual simulation are three-hour time history information. Where H_s is the significant wave height, T_p is the spectral peak period, "Shape" is the spectral shape parameter, H_{max} is the maximum wave height, and T_{pDir} is the wave direction. "Depth" is the depth from sea level, "Velocity" is the three-hour mean current speed, and "MeanDir" is the three-hour mean current direction relative to the bow.

3 Hydrodynamic numerical modelling of "NHTZ" FPS

Hydrodynamic numerical simulations, which are the principal analysis methods used in the design of marine engineering platforms, are based on the three-dimensional potential flow theory. The added mass matrix, damping matrix of the platform, and the response amplitude operator (RAO) of the platform motion, are obtained using frequency domain calculations. The results of the frequency domain calculations are then transformed into the time domain.

Table 2 Three-hour environmental load data under Condition 1

Wind	V(3hr@10m) (m/s)		MeanDir(3hr@10m) (°)
	15.56		61.80
Wave	H_s (m)		3.22
	T_p (s)		8.90
	Shape		1.67
	H_{max} (m)		5.38
	T_{pDir} (°)		44.00
Current	Depth (m)	Velocity (m/s)	MeanDir (°)
	6	0.66	−48.48
	7	0.68	−51.58
	8	0.69	−49.76
	9	0.68	−51.03
	10	0.68	−50.57
	11	0.69	−46.53
	12	0.70	−46.25
	13	0.69	−50.45
	14	0.69	−48.21
	15	0.70	−49.38
	16	0.66	−76.44
	17	0.64	−40.28

Table 3 Three-hour environmental load data under Condition 2

Wind	V(3hr@10m) (m/s)		MeanDir(3hr@10m) (°)
	10.12		87.68
Wave	H_s (m)		1.82
	T_p (s)		8.15
	Shape		1.67
	H_{max} (m)		3.03
	T_{pDir} (°)		72.49
Current	Depth (m)	Velocity (m/s)	MeanDir (°)
	6	0.47	282.24
	7	0.48	275.80
	8	0.49	274.43
	9	0.48	270.85
	10	0.49	271.61
	11	0.50	270.20
	12	0.49	284.68
	13	0.48	273.04
	14	0.48	278.81
	15	0.46	276.06
	16	0.45	270.69
	17	0.36	272.05

Finally, the platform motions under external loads can be obtained by the calculation in the time domain with the governing motion equation (Zhang et al., 2013) as follows:

$$(\boldsymbol{M}+\boldsymbol{M}_a)\ddot{\boldsymbol{X}}(t)+\boldsymbol{C}\dot{\boldsymbol{X}}(t)+\boldsymbol{K}\boldsymbol{X}(t)=\boldsymbol{F}_{wi}(t)+\boldsymbol{F}_{cu}(t)+\boldsymbol{F}_{wa}(t)+\boldsymbol{F}_{mo}(t), \tag{1}$$

where $\boldsymbol{M}$ is the mass matrix of the platform, $\boldsymbol{M}_a$ is the added mass matrix, $\boldsymbol{C}$ is the damping matrix, $\boldsymbol{K}$ is the stiffness matrix of the platform with the mooring system, $\boldsymbol{F}_{wi}$ is the wind load vector, $\boldsymbol{F}_{cu}$ is the current load vector, $\boldsymbol{F}_{wa}$ is the wave load vector, $\boldsymbol{F}_{mo}$ is the mooring restoring force vector and $\boldsymbol{X}$, $\dot{\boldsymbol{X}}$, and $\ddot{\boldsymbol{X}}$ are the displacement, velocity, and acceleration vectors, respectively.

According to the specifications reported in the platform design, this paper established a hydrodynamic model of the platform by using the hydrodynamics software AQWA. The parameters of the floating body and mooring system are shown in Table 4 and Table 5, respectively. The vessel model of the hydrodynamic simulation is given in Fig. 2, and the arrangements of the underwater mooring system are shown in Fig. 3.

The wind force and current force are obtained according to the wind force and current force coefficients using their respective calculation formulae as follows:

Table 4 Floating body parameters of "NHTZ" FPS

Parameters	Value	Parameters	Value
Draft (m)	22.86	Displacement (kg)	2.82×10^7
VCG from WL (m)	−1.585	Vessel weight (kg)	2.69×10^7
Roll gyradius (m)	29.29	Pitch gyradius (m)	29.23
Yaw gyradius (m)	33.44		

Table 5 Mooring system parameters of "NHTZ" FPS

Line segments	Grade	Length (m)	Wet weight (kg/m)	Drag coef.	Added mass
Platform chain	R4	221	276.80	2.45	1
Riser wire	SPIRAL STR.	503	71.30	1.20	1
Ground chain	R3	463−610	372.05	2.45	1
Anchor wire	SPIRAL STR.	122	71.30	1.20	1

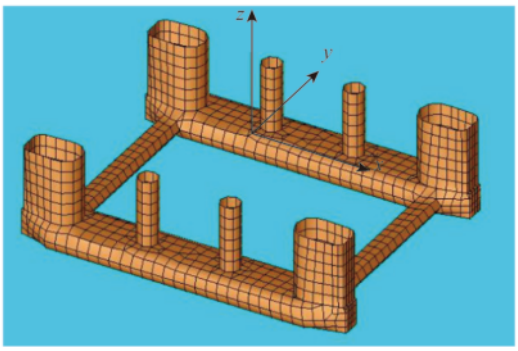

Fig. 2. Underwater structure model of "NHTZ" FPS.

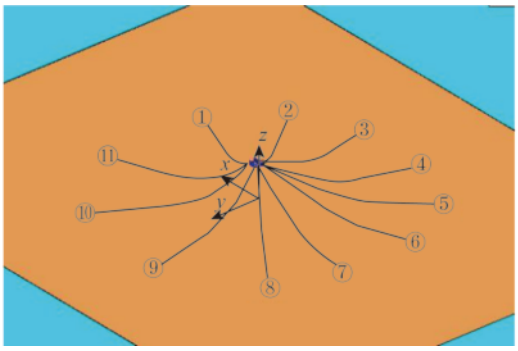

Fig. 3. Mooring system model of "NHTZ" FPS.

$$F_{\mathrm{wi}}(t)=\frac{1}{2}C_{\mathrm{wi}}\rho_{\mathrm{ai}}A_{\mathrm{wi}}v_{\mathrm{wi}}^2; \tag{2}$$

$$M_{\mathrm{wi}}(t)=\frac{1}{2}C_{\mathrm{wi}}\rho_{\mathrm{ai}}A_{\mathrm{wi}}v_{\mathrm{wi}}^2L_{\mathrm{wi}}; \tag{3}$$

$$F_{\mathrm{cu}}(t)=\frac{1}{2}C_{\mathrm{cu}}\rho_{\mathrm{wa}}A_{\mathrm{cu}}v_{\mathrm{cu}}^2; \tag{4}$$

$$M_{\mathrm{cu}}(t)=\frac{1}{2}C_{\mathrm{cu}}\rho_{\mathrm{wa}}A_{\mathrm{cu}}v_{\mathrm{cu}}^2L_{\mathrm{cu}}, \tag{5}$$

where F_{wi} and F_{cu} are the wind and current forces; M_{wi} and M_{cu} are the wind heeling and current heeling moments; C_{wi} and C_{cu} are the wind force and current force coefficients; ρ_{ai} and ρ_{wa} are the densities of air and sea water; A_{wi} and A_{cu} are the frontal and windward areas of the platform; v_{wi} and v_{cu} are the wind speed and current speed; and L_{wi} and L_{cu} are the lengths of the wind heeling and current heeling arms, respectively.

Wave force on the platform is calculated by combining the potential flow theory with the Morrison equation. Unidirectional or multiple directional second order drift forces are evaluated by the far-field solution, near field solution, or full quadratic transfer function (QTF) matrix. The QTF method is used in this paper to calculate second order drift forces. For constructing a model of ocean wave loads, wave spectral density analysis methods are commonly used. These include the P-M spectrum, ITTC single parameter spectrum, ITTC (ISSC) two parameter spectrum, JONSWAP spectrum, etc. Among them, the most widely used is the JONSWAP spectrum, for which the formula is as follows:

$$S(f)=\alpha H_{\mathrm{s}}^2T_{\mathrm{p}}^{-4}f^{-5}\exp[-1.25(T_{\mathrm{p}}f)^{-4}]\gamma^{\exp[-(T_{\mathrm{p}}f-1)^2/(2\sigma^2)]} \tag{6}$$

where f is the wave frequency, γ is the spectral parameter, σ is the peak shape parameter, and α is a constant related to the wind speed and fetch length.

$$\sigma=\begin{cases}0.09, & f\geqslant f_{\mathrm{p}}\\ 0.07, & f<f_{\mathrm{p}}\end{cases} \tag{7}$$

$$\alpha=\frac{0.0624}{0.230+0.0336\gamma-0.185/(1.9+\gamma)}. \tag{8}$$

Jin et al. (2015) considered the statistical analysis of the wave monitoring data in "NHTZ" FPS and found that the measured wave spectrum was closer to the JONSWAP spectrum than any other. Based on a least square estimation of γ for the JONSWAP spectrum, the wave spectrum parameter γ is 1.67.

The second-order wave force in this paper is calculated by QTF. An example of QTF with six degrees of freedom in 45° direction is given (see Fig. 4).

Fig. 5 presents the comparisons of RAOs from the hydrodynamic model and those based on the platform design, at the wave force angles of 0°, 45°, and 90°. The comparisons showed that the RAOs derived from the hydrodynamic models were in good agreement with the RAOs based on the design indicators of the platform, showing that

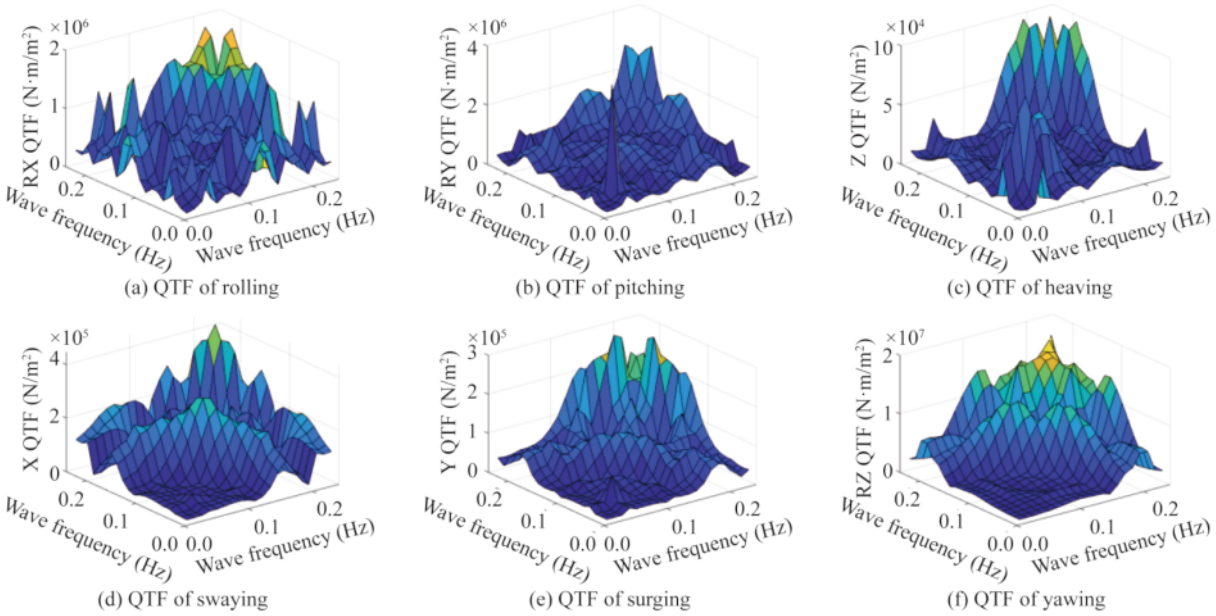

Fig. 4. QTF of the 6-DOF.

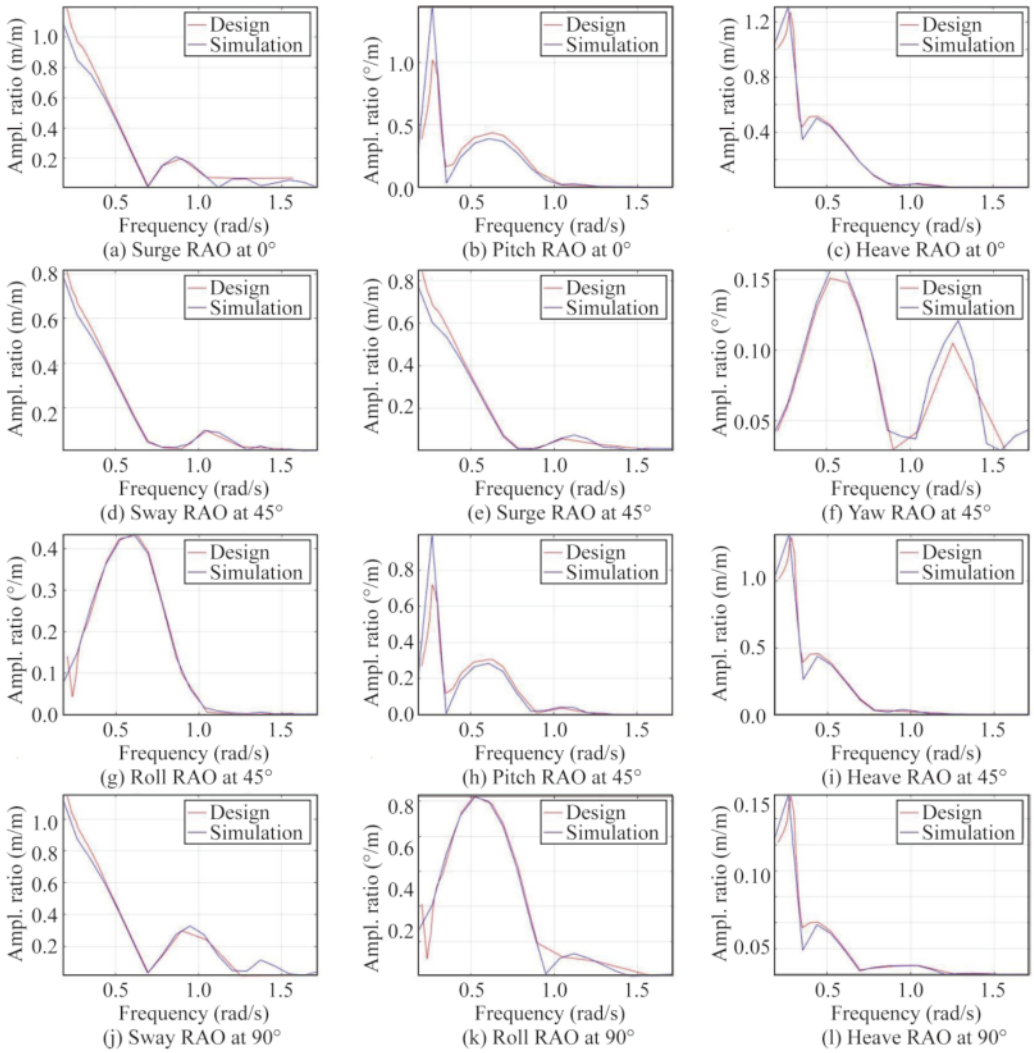

Fig. 5. RAO comparison diagram of the 6-DOF.

the platform hydrodynamic model and the platform were consistent.

The load data of the two sets of sea conditions were input into the hydrodynamic model, and simulations using the two sets of sea conditions were conducted. Fig. 6 shows a comparison of the simulated hydrodynamic time series and the corresponding field of measured 6 DOF time series.

4 Comparisons of measured and simulated data

The statistics of the motion time series directly characterize the motion characteristics of the offshore platform. By analyzing the statistical values, the platform's range of motion can be determined and the response extremes can be identified. Meanwhile, a frequency spectrum analysis of the dynamic response of the platform can be made to investigate the motion period, the main components of the motions, and the coupled behaviors of each motion. This paper compared the amplitudes, distribution characteristics, reciprocating times, and spectrum characteristics of the 6 DOF motion responses of the platform.

4.1 Comparisons of 6 DOF motion extremes

The maximum values of the measured and simulated 6 DOF motions were obtained for this comparison. Table 6 lists the extremes from the hydrodynamic simulations and the measured data under the two sets of sea conditions, and a histogram of this comparison is shown in Fig. 7.

From the extremes of the hydrodynamic simulation and

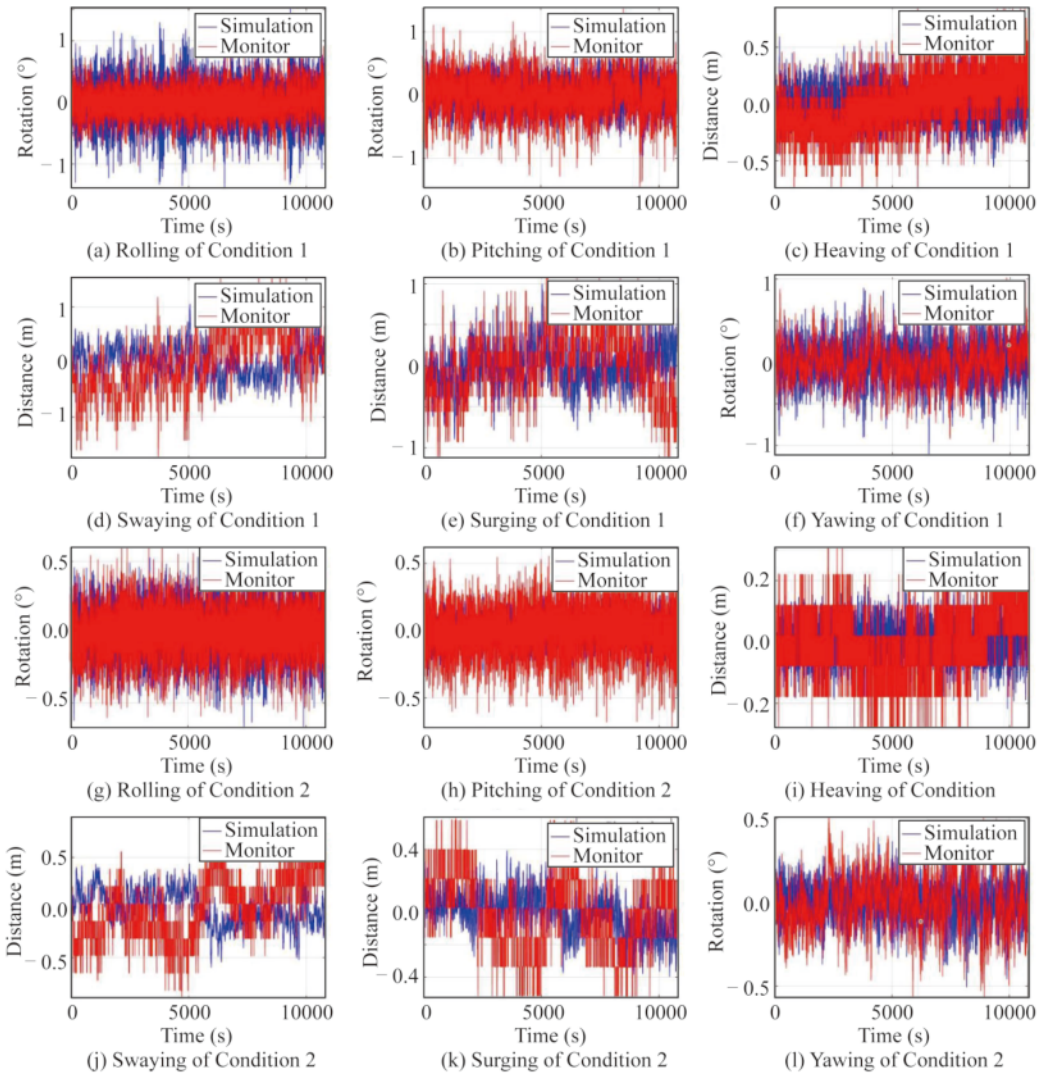

Fig. 6. Simulated and measured motion time series under two working conditions.

Table 6 Amplitude error under two conditions

	Error					
	Sway	Surge	Yaw	Roll	Pitch	Heave
Condition 1	38.3%	12.8%	−6.1%	−2.8%	15.2%	26.0%
Condition 2	42.8%	32.1%	9.9%	−3.4%	47.6%	26.5%

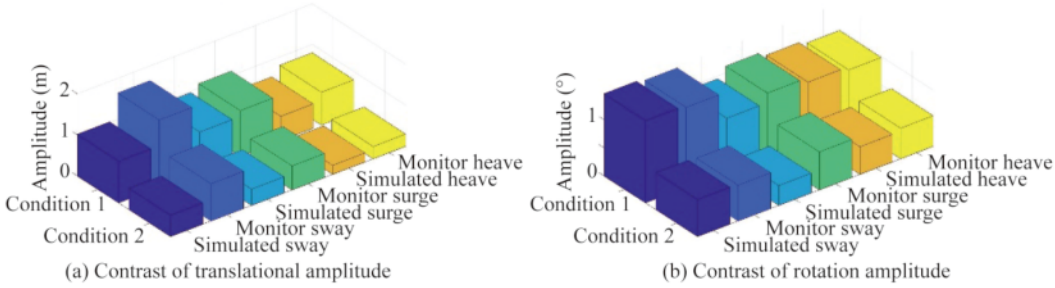

Fig. 7. Motion amplitude comparison of the two conditions.

measured data, it can be seen that there was only a small difference in the roll responses, while there were large differences in the translational DOFs such as sway, surge, and heave. Furthermore, the results from the hydrodynamic simulations were generally smaller than the measured results. This was because hydrodynamic simulations of marine structures depend heavily on the Morison formula and potential flow theory which use first-order approximations of velocity potential. To counter this bias, more attention should be paid to the influence of slow drift forces of the second-order on the motions of the platform.

4.2 Comparative analysis of the distributions of rotational DOFs

In order to better fit the distribution law of the translational DOF, Gaussian smoothing is performed on the translational DOF data. It was found that, under the two sea conditions, the distributions of the 6 DOF of the platform conformed to the normal distribution. The fitting results are shown in Fig. 8.

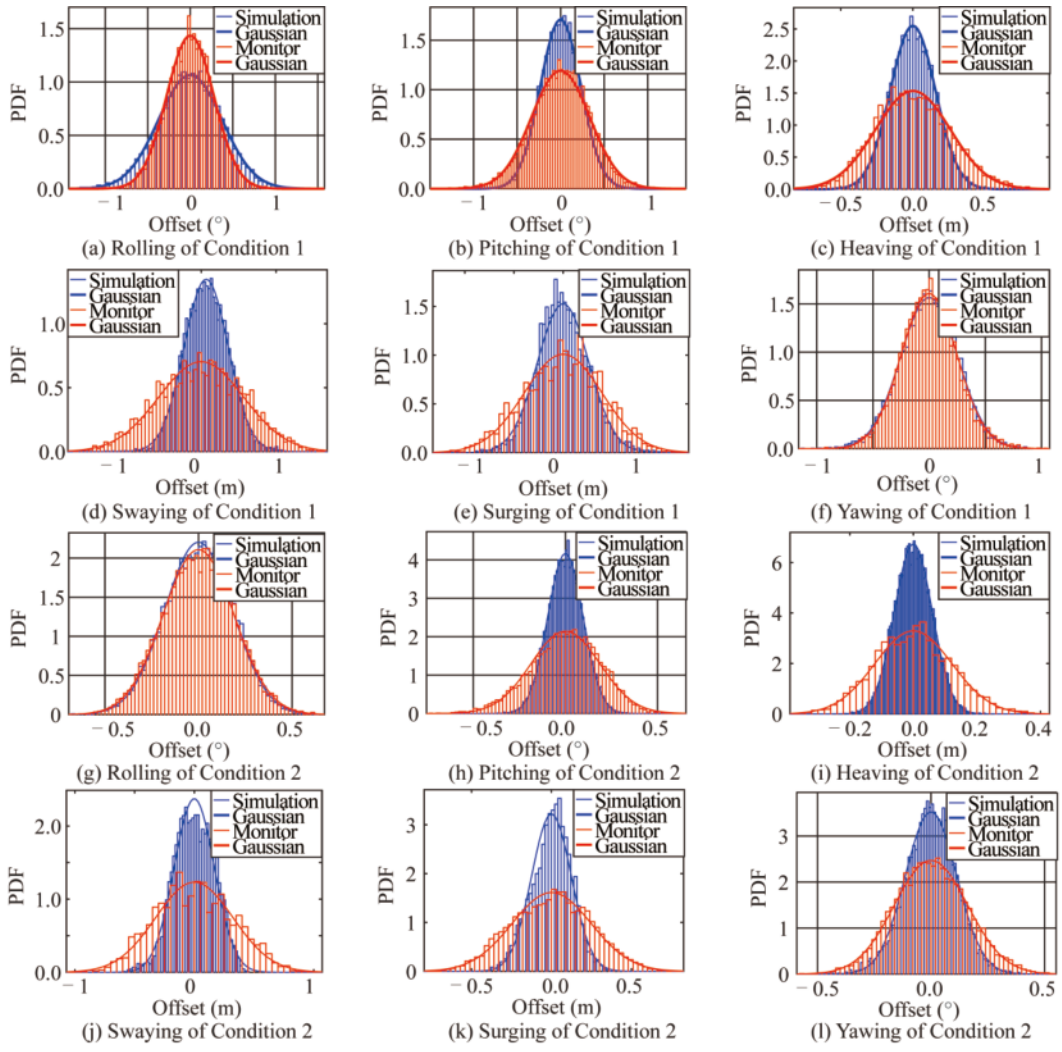

Fig. 8. Fit of 6 DOF distributions under two environmental conditions.

According to the properties of the normal distribution, the differences between the measured 6 DOF and the simulation results also obeyed the normal distribution. This can provide evidence for the construction of the likelihood function when updating model based on Bayesian distribution (Beck and Katafygiotis, 1998).

4.3 Comparison of reciprocating number of 6 DOF motions

By analyzing the reciprocating motion of the 6 DOF during the 3 hour periods under the two environmental conditions, the number of motion cycles and motion amplitudes of each DOF were obtained as shown in Fig. 9 and Table 7. The width of bin is the accuracy of sensor.

According to the results, the total number of cycles was less when the sea conditions were worse. With the exception of heaving motion, the number of cycles in the measured data was greater than that in the simulated results. For example, the number of effective cycles of sway and surge in the measured data was 44% larger than that in the simulated data, and the difference was mainly due to differences in the wave period component. The number of effective cycles of the rotational DOF in the measured data was 21% larger

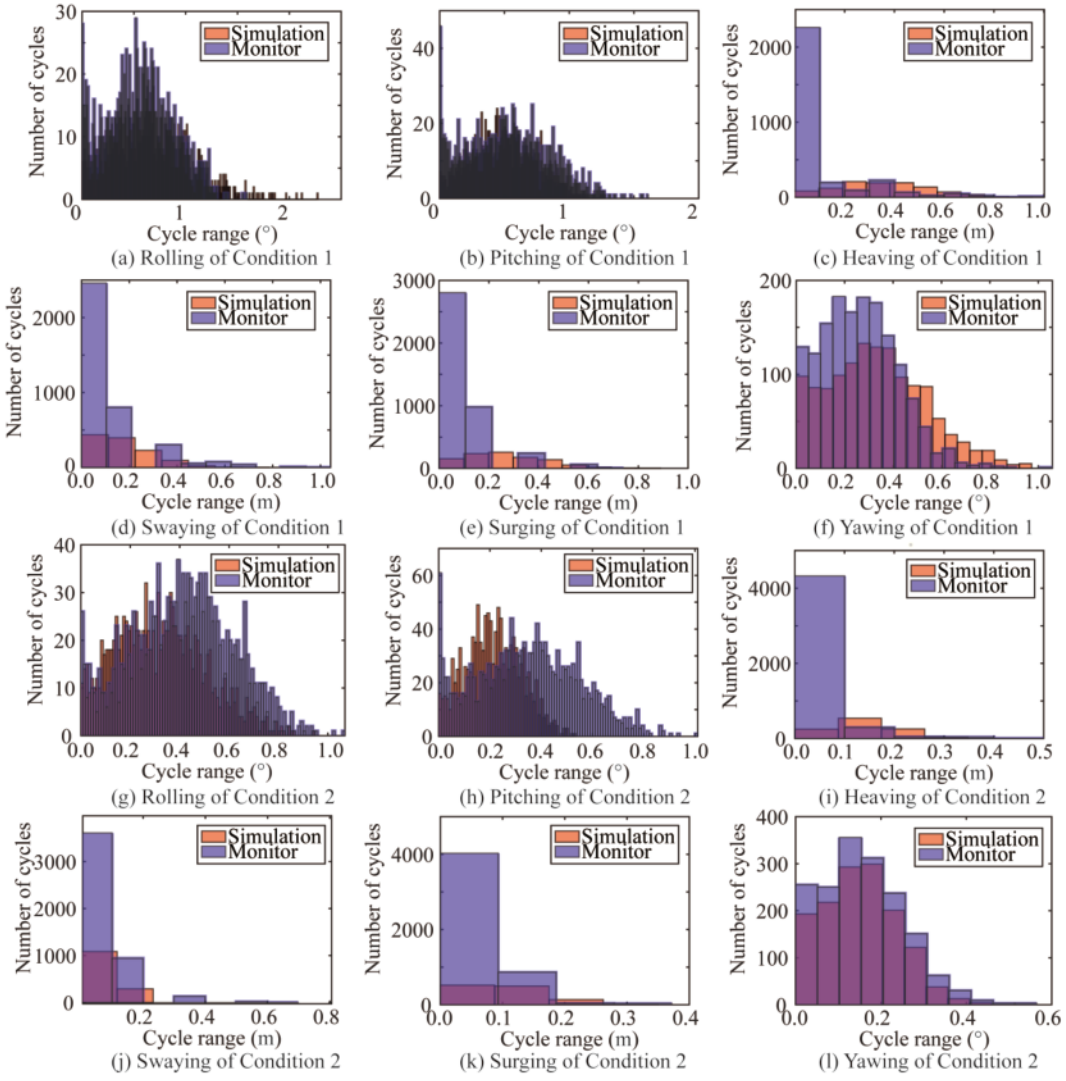

Fig. 9. Number of motion cycles for the 6-DOF under the two conditions.

Table 7 Total number of cycles under two conditions

	Monitored sway	Simulated sway	Monitored surge	Simulated surge	Monitored heave	Simulated heave
Condition 1	1276	744	1281	888	670	960
Condition 2	1090	285	929	643	378	825
	Monitored roll	Simulated roll	Monitored pitch	Simulated pitch	Monitored yaw	Simulated yaw
Condition 1	1450	1132	1462	1128	1407	1217
Condition 2	1543	1173	1649	1156	1413	1188

than that in the simulated data. These observations showed that when using hydrodynamic analysis to inform the design of platforms, the number of motion cycles of the platform will be underestimated, which will result in overestimates of lifespans of the floating body, moorings, risers, and other components, putting the platform and its occupants at risk.

4.4 Comparison in the spectrum domain

Spectral analyses are conducted to study time series data in the frequency domain, and are often applied to the study of the frequency components of a dynamic system. If the auto-correlation function of random signal $x(t)$ is $R_x(\tau)$, then the Fourier transform of $R_x(\tau)$ is as follows:

$$S_x(f) = \int_{-\infty}^{+\infty} R_x(\tau) \mathrm{e}^{-\mathrm{j}2\pi f\tau} \mathrm{d}\tau, \tag{9}$$

where $S_x(f)$ is defined as the power spectrum density of $x(t)$ and $S_x(f)$ can be interpreted as the distribution function of the average power of $x(t)$ relative to frequency. The power spectrum $S_x(f)$ contains all the information of $R_x(\tau)$. If the signal contains a frequency component, it can be extracted from the power spectrum. Indeed, the purpose of power spectrum estimation is to describe the distribution of the frequency component of the signal based on limited data. The power spectra of the 6 DOF motions are given in Fig. 10.

It can be seen that the main difference in the frequency components of the 6 DOF motions between the measured monitoring data and the hydrodynamic simulation appeared in the low-frequency portion. This showed that the hydrodynamic simulation underestimated the low-frequency, large-amplitude motion of the platform. This agreed with Stansberg (2007), who pointed out that the slow drift motion was difficult to account for. Therefore, the influence of the slow drift motion on the performance of the platform should be given more attention during the design stage. It was noteworthy that the slow drift to pitch motion was not only significant, but also its amplitude was essentially the same as the wave frequency. Therefore, the influence of slow drift increased with increasing severity of the sea state. The slow drift motion also made a large contribution to heave motion, but in this case its amplitude was larger than that of the wave

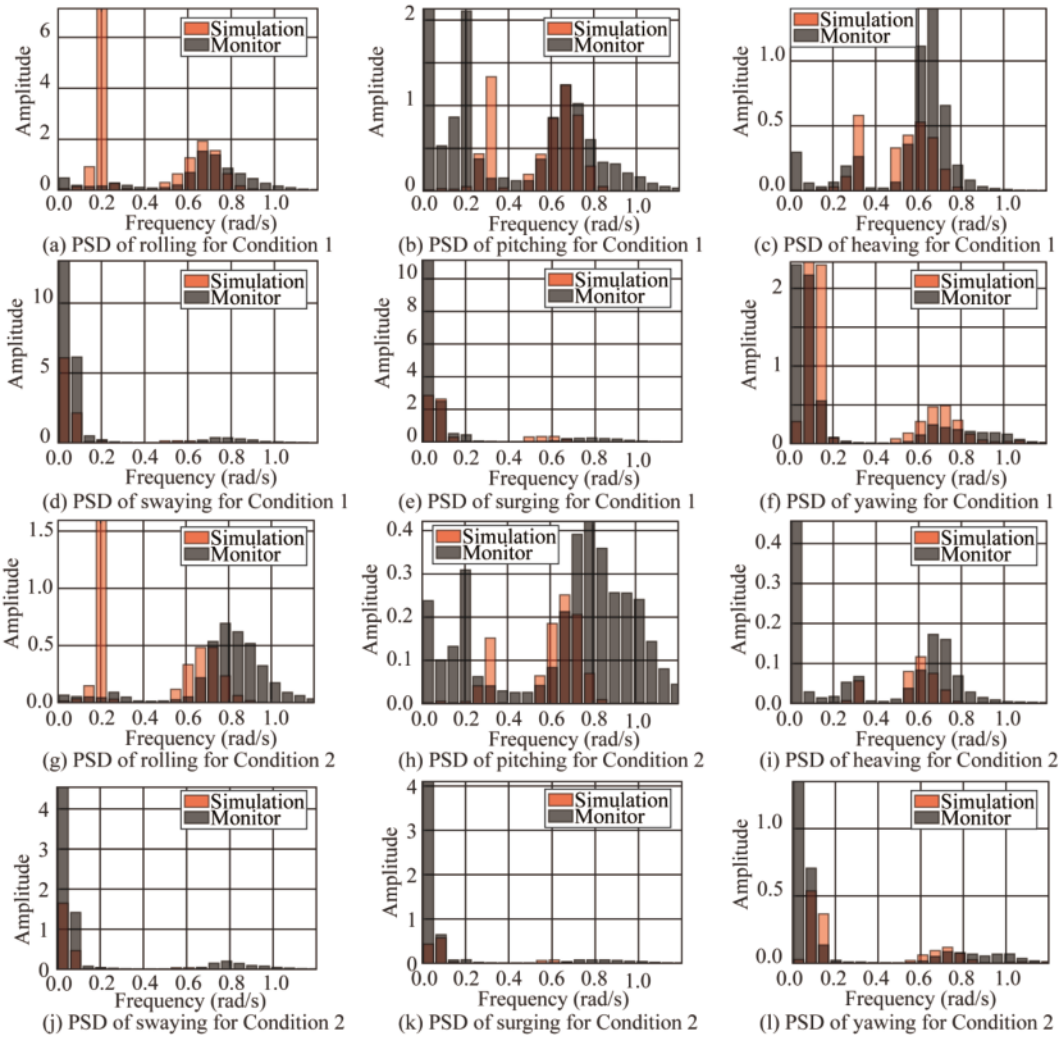

Fig. 10. Spectrum diagram of the motion of the 6-DOF.

frequency. The excitation mechanisms of slow drift motion include second-order wave drift torque, the torque of wind and current, and the coupled behavior of heave and pitch.

In order to further analyze the composition of each frequency extracted from the dynamic response, the empirical mode decomposition (EMD) of the 6-DOF was carried out. EMD is a new method to deal with both non-stationary and nonlinear data by decomposing it. It is an intuitive, direct, and adaptive method based on decomposition which is based on and derived from the data. In the EMD theory, several intrinsic oscillation modes that depend on the complexity of data coexist in the data at the same time. These modes can be empirically identified by their characteristic time scales in the data. The time series are decomposed into finite sets of intrinsic mode functions (IMFs) and residuals are obtained based on the local minima and maxima (Flandrin and Gonçalvès, 2004). Taking the relatively severe seas of Condition 1 as an example, we first analyzed the correlations between the IMFs of each order obtained from the EMD and the original signal. The IMFs whose correlation coefficients were smaller than 0.1 were eliminated. Then the power spectrum of each IMF was calculated. Fig. 11 presents the IMF decomposition results and the corresponding power spectra of the 6 DOF motions under two sets of sea conditions.

It can be seen from the comparison that the 6 DOF motion responses were composed mainly of the low-frequency slow drift motion, wave-induced excitation, and the motion coupled with the natural period of the platform. The periods of the sway, surge, and yaw of "NHTZ" FPS ranged between 54–78 s, and the periods of roll, pitch, and heave ranged within 19–36 s. Notably, the IMF results demonstrated that the measured sway motion had the periodic component of roll, and the measured roll and pitch motions had the periodic components of sway and surge. This phenomenon was not obvious in the hydrodynamic simulation results. This indicated that there was an obvious coupling between the translational DOF and rotational DOF of the platform, but the hydrodynamic numerical modelling process could not fully characterize this behavior.

As can be seen from the above, there are some differences between the hydrodynamically simulated results and the prototype measured data. The reasons of the differences can be explained as follows. First and the foremost, due to the long-term service of the platform, the designed parameters have been changed, resulting in the service platform param-

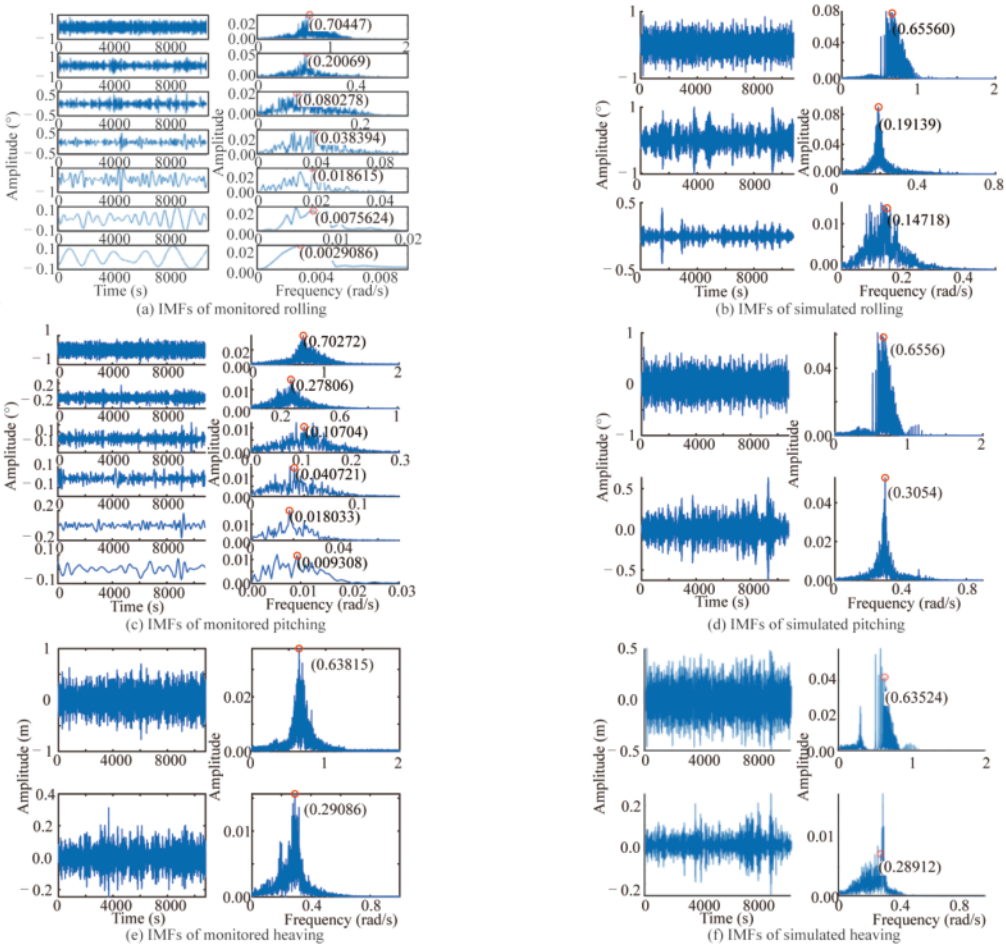

Fig. 11. IMFs and power spectra of the 6 DOF motions (continued on next page).

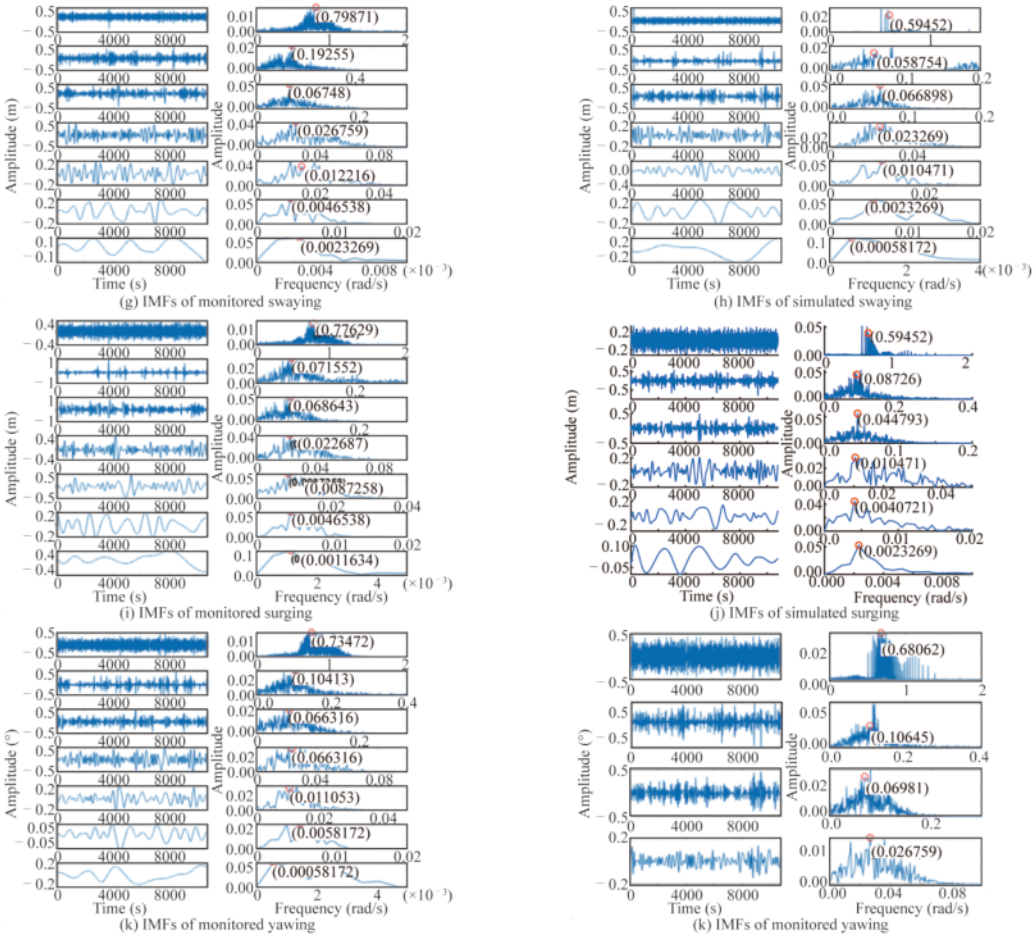

Fig. 11. (continued).

eters being different from the original ones. Second, the first-order and second-order wave forces are considered in the hydrodynamic simulation process of AQWA software, while the actual process of waves includes the influence of higher-order wave forces. Furthermore, the simplification of the ocean environmental loads and the empirical values of the additional mass coefficients and drag force coefficients in hydrodynamic modeling lead to the inconsistency between the simulated and measured process. The model parameter modification and ocean environmental loading models should be paid more attention to in the next research.

5 Conclusions

In this paper, based on the data from a prototype monitoring system installed on the "NHTZ" FPS, the performance of a hydrodynamic numerical simulation was assessed by comparing it with the measured results. The following conclusions were made.

(1) The hydrodynamic simulation correctly reproduced the motion behavior of the 6 DOF motion responses of the platform. Compared with the field measured data, the hydrodynamic simulation can reproduce the motion behavior of the platform with good accuracy in the frequency domain. The amplitudes of the hydrodynamic simulation were smaller than those of the measured results.

(2) The hydrodynamic numerical simulation underestimated the reciprocating motion of the 6 DOF responses of platform. The reciprocating motion of the translational DOF was underestimated by 44%, and that of the rotational DOF was underestimated by 21%. Underestimating the reciprocating motion of the 6 DOF will produce overestimations of the lifespans of structural components.

(3) The simulation also underestimated the influence of slow drift on the motions of the platform. The measured data showed that slow drift made a significant contribution to pitch motion, and its contribution to the platforms motion increased under harsh sea conditions.

(4) The 6 DOF motions of the platform include the low-frequency slow drift motion, the coupled motion with the natural period of the structure, and wave-induced excitations. The measured roll, sway, pitch and surge all showed evidence of coupled motion behavior. The hydrodynamic numerical simulation underestimated this behavior.

References

Asadollahi, P. and Li, J., 2017. Statistical analysis of modal properties of a cable-stayed bridge through long-term wireless structural health

monitoring, *Journal of Bridge Engineering*, 22(9), 04017051.1.

Beck, J.L. and Katafygiotis, L.S., 1998. Updating models and their uncertainties. I: Bayesian statistical framework, *Journal of Engineering Mechanics*, 124(4), 455–461.

Brownjohn, J.M.W., Koo, K.Y., Scullion, A. and List, D., 2015. Operational deformations in long-span bridges, *Structure and Infrastructure Engineering*, 11(4), 556–574.

Chen, B.C., Mu, T.M., Chen, Y.Y. and Huang, J.Z., 2013a. State-of-the-art of research and engineering application of steel-concrete composite bridges in China, *Journal of Building Structures*, 34(S1), 1–10. (in Chinese)

Chen, Y.N., Chen, G. and Xiao, L.F., 2013b. Calculation and analysis of second-order force and slow drift damping in shallow water FPSO, *Proceedings of the 16th China Ocean* (*Coastal*) *Engineering Adademic Seminars*, Dalian, pp. 45–52. (in Chinese)

Clauss, G.F., Schmittner, C.E. and Stutz, K., 2003. Freak wave impact on semisubmersibles-time-domain analysis of motions and forces, *Proceedings of the Thirteenth International Offshore and Polar Engineering Conference*, The International Society of Offshore and Polar Engineers, Honolulu, pp. 1794–1801.

Du, Y., Wu, W.H., Tang, D., Yue, Q.J., Li F. and Xie, R.B., 2015. A novel underwater measurement method for mooring system using self-contained technique, *Advances in Mechanical Engineering*, 7(5), doi: 10.1177/1687814015585973.

Du, Y., Wu, W.H., Wang, Y.L. and Yue, Q.J., 2014. Prototype Data Analysis on LH11–1 Semisubmersible Platform in South China Sea, *Proceedings of the ASME 2014 33rd International Conference on Ocean*, *Offshore and Arctic Engineering*, ASME, San Francisco, pp. 2–15.

Du, Y., Wu, W.H. and Yue, Q.J., 2013. Prototype measurement for deep water floating platforms based on monitoring technology, *Proceedings of the ASME 2013 32nd International Conference on Ocean*, *Offshore and Arctic Engineering*, ASME, Nantes.

Du, Y., Wu, W.H., Yue, Q.J., Shi, Z.M., Li F., Xie, R.B. and Huang, D., 2016. Prototype monitoring technique for deep water floating platform, *Journal of Shanghai Jiaotong University*, 50(3), 448–455. (in Chinese)

Edwards, R., Prislin, I., Johnson, T., Campman, C. and Leverette, S., 2005. Review of 17 real-time, environment, response, and integrity monitoring systems on floating production platforms in the deep waters of the Gulf of Mexico, *Proceedings of Offshore Technology Conference*, OTC, Houston, pp. 1990–2005.

Feng, W., Du, Q.G., Li, X.K., Su J., Yan, B., Zhu, Z.Y. and Song, L.S., 2015. The selection of typical loading cases for motion analysis of a semi-submersible drilling platform, *China Offshore Platform*, 30(1), 84–89, 95. (in Chinese)

Flandrin, P. and Gonçalvès, P., 2004. Empirical mode decompositions as data-driven wavelet-like expansions, *International Journal of Wavelets*, *Multiresolution and Information Processing*, 2(4), 477–496.

Halkyard, J., Liagre, P. and Tahar, A., 2004. Full scale data comparison for the horn mountain spar, *Proceedings of the ASME 2004 23rd International Conference on Offshore Mechanics and Arctic Engineering*, ASME, Vancouver, pp. 1123–1132.

Hunt, S.R. and Hebden, I.G., 1999. Eurofighter 2000: An integrated approach to structural health and usage monitoring, *Proceedings of the 19th Symposium of the International-Committee-on-Aeronautical-Fatigue–Fatigue in New and Ageing Aircraft* (*ICAF 97*), pp. 481–498.

Hunt, S.R. and Hebden, I.G., 2001. Validation of the Eurofighter Typhoon structural health and usage monitoring system, *Smart Materials and Structures*, 10(3), 497–503.

Jin, Y., Wu, W.H., Du, Y., Feng, J.G. and Li, P., 2015. Analysis of motion characteristics of "Nanhai Tiao Zhan" semi-submersible platform in measured environment, *Proceedings of the 17th China Ocean* (*Coastal*) *Engineering Adademic Seminars*, China Ocean Press, Nanning, pp. 6. (in Chinese)

Kim, S., Park, J. and Kim, H.K., 2017. Damping identification and serviceability assessment of a cable-stayed bridge based on operational monitoring data, *Journal of Bridge Engineering*, 22(3), 04016123.

Ko, J.M. and Ni, Y.Q., 2005. Technology developments in structural health monitoring of large-scale bridges, *Engineering Structures*, 27(12), 1715–1725.

Leverette, S., Rijken, O., Dooley, W. and Thompson, H., 2003. Analysis of TLP VIV responses to eddy currents, *Proceedings of the Offshore Technology Conference*, OTC, Houston, pp. 1947–1954.

Low, Y.M. and Langley, R.S., 2006. Time and frequency domain coupled analysis of deepwater floating production systems, *Applied Ocean Research*, 28(6), 371–385.

Pedersen, E.A., 2012. *Motion Analysis of Semi-Submersible*, Bjǫrnar Pettersen, IMT.

Perego, R.N., Li, G., Beynet, P.A., Chappell, J.F., Garrett, D.L. and Gordon, R.B., 2005. The Marlin TLP: Measured and predicted responses during hurricane Ivan, *Proceedings of Offshore Technology Conference*, OTC, Houston, pp. 971–979.

Senra, S.F., Correa, F.N., Jacob, B.P., Mourelle, M.M, and Masetti, I. Q., 2002. Towards the integration of analysis and design of mooring systems and risers: Part I–studies on a semisubmersible platform, *Proceedings of the ASME 2002 21st International Conference on Offshore Mechanics and Arctic Engineering*, ASME, Oslo, pp. 41–48.

Söylemez, M. and Atlar, M., 2000. A comparative study of two practical methods for estimating the hydrodynamic loads and motions of a semi-submersible, *Journal of Offshore Mechanics and Arctic Engineering*, 122(1), 57–63.

Stansberg, C.T., 2007. Slow-drift pitch motions and air-gap observed from model testing with moored semisubmersibles, *Proceedings of the ASME 2007 26th International Conference on Offshore Mechanics and Arctic Engineerin*g, ASME, San Diego, pp. 659–668.

Tahar, A., Finn, L., Liagre, P. and Halkyard, J., 2005. Full scale data comparison for the horn mountain spar mooring line tensions during hurricane Isidore, *Proceedings of the ASME 2005 24th International Conference on Offshore Mechanics and Arctic Engineering*, ASME, Halkidiki, pp. 891–899.

Tahar, A., Halkyard, J. and Irani, M., 2006. Comparison of time and frequency domain analysis with full scale data for the horn mountain spar during hurricane Isidore, *Proceedings of the 25th International Conference on Offshore Mechanics and Arctic Engineering*, ASME, Hamburg, pp. 105–113.

Teigen, P. and Haver, S., 1998. The Heidrun TLP: Measured versus predicted response, *Applied Ocean Research*, 20(1-2), 27–35.

US Department of Defense, 2020. *UFC 4-159-03 Moorings*, US Department of Defense, New York.

van Sluijs, M.F. and Minkenberg, H.L., 1977. A review of studies of ocean platform motions, *Ocean Engineering*, 4(2), 75–90.

Wang, H., Zhang, Y.M., Mao, J.X., Wan, H.P., Tao, T.Y. and Zhu Q. X., 2019. Modeling and forecasting of temperature-induced strain of a long-span bridge using an improved Bayesian dynamic linear model, *Engineering Structures*, 192, 220–232.

Yang, H., Liu, B., Zhang, G.L., et al., 2012. Motion analysis and weather window selection for towing of "Nan Hai Tiao Zhan" semisubmersible platform, in: Duan, M.L. (ed.), *Proceedings of SUT International Conference on Subsea Technology and Deepwater*

Engineering (*2012*), Petroleum Industry Press, Beijing, pp. 72–79. (in Chinese)

Zhang, R.Y., Tang, Y.G., Hu, J., Ruan, S.F. and Chen, C.H., 2013. Dynamic response in frequency and time domains of a floating foundation for offshore wind turbines, *Ocean Engineering*, 60, 115–123.